UC Irvine
UC Irvine Previously Published Works

Title

PER2 Controls Lipid Metabolism by Direct Regulation of PPARγ

Permalink

https://escholarship.org/uc/item/6zj434ss

Journal

Cell Metabolism, 12(5)

ISSN

1550-4131

Authors

Grimaldi, Benedetto
Bellet, Marina Maria
Katada, Sayako
et al.

Publication Date

2010-11-01

DOI

10.1016/j.cmet.2010.10.005

Copyright Information

Peer reviewed

PER2 Controls Lipid Metabolism by Direct Regulation of PPARγ

Benedetto Grimaldi[1], **Marina Maria Bellet**[1], **Sayako Katada**[1], **Giuseppe Astarita**[1], **Jun Hirayama**[1], **Rajesh H. Amin**[2], **James G. Granneman**[3], **Daniele Piomelli**[1], **Todd Leff**[2], and **Paolo Sassone-Corsi**[1,*]

[1] Department of Pharmacology, University of California, Irvine, Irvine, California 92697

[2] Department of Pathology, Wayne State University, Detroit, MI 48201

[3] Department of Psychiatry and Behavioral Neurosciences, Wayne State University, Detroit, MI 48201

Abstract

Accumulating evidence highlights intriguing interplays between circadian and metabolic pathways. We show that PER2 directly and specifically represses PPARγ, a nuclear receptor critical in adipogenesis, insulin sensitivity and inflammatory response. PER2-deficient mice display altered lipid metabolism, with drastic reduction of total triacylglycerol and non-esterified fatty acids. PER2 exerts its inhibitory function by blocking PPARγ recruitment to target promoters and thereby transcriptional activation. Whole-genome microarray profiling demonstrates that PER2 dictates the specificity of PPARγ transcriptional activity. Indeed, lack of PER2 results in enhanced adipocyte differentiation of cultured fibroblasts. PER2 targets S112 in PPARγ, a residue whose mutation has been associated to altered lipid metabolism. Lipidomic profiling demonstrates that PER2 is necessary for normal lipid metabolism in white adipocyte tissue. Our findings support a scenario in which PER2 controls the pro-adipogenic activity of PPARγ by operating as its natural modulator, thereby revealing potential avenues of pharmacological and therapeutic intervention.

INTRODUCTION

Circadian rhythms dominate most aspects of our metabolism and physiology. Circadian clocks are intrinsic, time tracking systems enabling organisms to anticipate environmental changes, thereby adapting their behavior and physiology to the appropriate time of day (King and Takahashi, 2000). While the anatomical center of the mammalian circadian clock resides in the suprachiasmatic nucleus (SCN), most peripheral tissues contain intrinsically independent pacemakers (Schibler and Sassone-Corsi, 2002). This property, coupled with the notion that the transcription of about 10% of all cellular genes oscillates in a circadian

manner (Akhtar et al., 2002) (Duffield et al., 2002) (Panda et al., 2002), underscores how profoundly the circadian transcriptional machinery influences a wide array of cellular functions.

At molecular level the circadian clock is based on interconnected transcriptional–translational feedback loops in which specific clock proteins repress transcription of their own genes (Young and Kay, 2001) (Reppert and Weaver, 2002). Various proteins compose the circadian clock, including three Period (PER1, PER2 and PER3), two Cryptochromes (CRY1 and CRY2), CLOCK and two BMAL proteins. Although highly similar in structure, the three mammalian proteins PER1, PER2 and PER3 appear to be functionally distinct (Lee et al., 2004) and their expression to be differentially regulated (Zylka et al., 1998) (Field et al., 2000). Clock-controlled gene (CCG) promoters contain E-box elements which mediate CLOCK-BMAL1 binding and transactivation (Reppert and Weaver, 2002). The CLOCK-BMAL1-mediated transcription of many CCGs reinforces the influence that the circadian molecular machinery has on a number of physiological processes. The result of this complex network of regulatory pathways is the circadian rhythmicity of many physiological processes, such as food intake and several aspects of metabolism. Increasing evidence links the circadian clock to cellular energy balance in various organisms (Eckel-Mahan and Sassone-Corsi, 2009).

Disruption of clock regulation leads to a number of pathological conditions, including metabolic disorders and increased susceptibility to cancer (Sahar and Sassone-Corsi, 2009). Presence of peripheral oscillators suggests that tissue-specific regulatory pathways may establish specialized connections with the clock machinery (Schibler and Sassone-Corsi, 2002). Moreover, clock regulators appear to be intimately implicated in cellular functions other than circadian control, thereby influencing cellular metabolism, cell cycle and cell proliferation (Wijnen and Young, 2006).

We hypothesize that *bona fide* clock regulators may operate within given transcriptional pathways in addition to their circadian function. Using both molecular and biochemical approaches we demonstrate that PER2 is a natural regulator of PPARγ transcriptional activity and it functions as a critical regulator of lipid metabolism.

RESULTS

Altered Lipid Metabolism in *Per2*-null Mice

While studying the relationship between circadian genes and metabolism, we noted that adult mice homozygous for targeted disruption of *Per2* (*Per2*^{-/-} mice; (Bae et al., 2001)) fed a standard diet weighed significantly less than their WT control siblings (Figure 1A). To examine if this difference could be age-related, we performed a growth curve analysis of *Per2*^{-/-} and WT littermates (Figure S1A). *Per2*^{-/-} male mice were considerably heavier during the pre-adolescence period (postnatal day (pnd) 23–35); during adolescence (pnd 36-48) *Per2*^{-/-} animals slowed down their growth rate until approximately the adult age (pnd >61), at which time they become progressively and significantly lighter than WT littermates. After around 4 months, the weight in the two genotypes remained consistently different

(Figure S1A). *Per2* deletion also results in a remarkable reduction in epididymal fat pad mass of adult mice (Figure 1B).

We further analyzed the whole-body composition of *Per2*^{-/-} animals by magnetic resonance imaging (MRI). This analysis revealed a 40% reduction in the fat/lean ratio in *Per2*^{-/-} mice (Figures 1C and 1D). Furthermore, mutant mice showed a drastic decrease in plasma levels of total triacylglycerol (TGA) and non-esterified fatty acid (NEFA) (Figures 1E and 1F). These alterations could not be attributed to differences in food intake, as food consumption was identical in *Per2*^{-/-} and WT mice (Figure 1G). When analyzed by indirect calorimetry, *Per2*^{-/-} mice showed a significant increase in oxygen consumption as compared to WT (Figure 1H). These results demonstrate a pronounced alteration of lipid metabolism in mice lacking the *Per2* gene.

As *Per2* is a bona fide clock gene, we reasoned that the altered lipid metabolism displayed by the *Per2*^{-/-} mice could derive from an aberrant circadian regulation. However, *Per2*^{-/-} mice kept under a regular light/dark cycle showed negligible differences in motor behavior and no overt circadian dysfunction in the SCN (Bae et al., 2001). We then compared the expression profile for circadian-regulated genes in white adipose tissue (WAT) from WT and *Per2*^{-/-} mice. Remarkably, *Dbp* and *Per1* circadian expression was virtually identical in WT and *Per2*^{-/-} mice (Figure 1I), indicating that the alteration in lipid metabolism is uncoupled from disruption of the circadian cycle.

To explore the mechanisms underlying the metabolic phenotype of *Per2*-null mice, we carried out a mass spectrometry (MS) analysis to identify PER2 interacting proteins. We reasoned that the carboxy-terminal region (aa 882-1257) would be the most appropriate portion to identify specific PER2-interacting proteins as it shares low degree of homology with other mammalian PERs and lacks the PAS domains (Hirayama and Sassone-Corsi, 2005). A tagged C-terminal PER domain was transiently expressed in human choriocarcinoma JEG-3 cells, whose transfection efficiency is higher than the adipogenic model 3T3-L1 cells (Schwarz et al., 1997). This analysis revealed that the C-terminal domain of PER2 prominently interacts with two proteins, the peroxisome proliferation activated receptor γ2 (PPARγ2) and HSPA8 (see full set of data in Table S1). Because of the phenotype of *Per2*-null mice, PPARγ2, a master regulator of adipogenic differentiation and lipid metabolism (Tontonoz and Spiegelman, 2008) (Lehrke and Lazar, 2005) attracted our attention.

PER2 Specifically Interacts with PPARγ and Represses its Transcriptional Activity

To study the association of PER2 with PPARγ, we first confirmed that the native PER2 and PPARγ proteins interact *in vivo* by co-immunoprecipitating those from WAT (Figure 1J). We then performed co-IP assays from cultured cells transiently expressing a Flag-PPARγ protein and different tagged-components of the clock machinery. This analysis confirmed the MS results and revealed that PER2 is the only clock protein able to interact with PPARγ (Figure 1K). We also found that PER2 associates with equal efficacy with the two PPARγ1 and PPARγ2 isoforms (Figure S1B). Notably, PER1, which presents a high degree of homology with PER2, did not interact with PPARγ (Figure 1K), suggesting the presence in PER2 of a specific and yet unidentified PPARγ-interaction domain.

PER2 inhibits CLOCK:BMAL1-driven transcription by dimerizing with the powerful repressor CRY (King and Takahashi, 2000). We explored whether PER2 regulates PPARγ–induced transcription of a PPAR-driven reporter. As previously reported (Lehmann et al., 1995), increasing doses of the selective PPARγ agonist, rosiglitazone, produced a concentration-dependent increase in transcriptional activation (Figure 1L). Co-expression of PER2 resulted in a marked reduction of PPARγ-dependent transcription, even at the highest concentrations of rosiglitazone. This represents an interesting case of control exerted by a clock protein on a transcriptional activator that does not operate within the core circadian regulatory system.

In contrast to PER2, other clock proteins – including the powerful repressor CRY1 – produced negligible changes in PPARγ-mediated transcriptional activity (Figure 1M). Importantly, CRY1 does not enhance the repressive function of PER2 on PPARγ (Figure S1C), and the effect of PER2 on PPARγ is CRY-independent, as demonstrated by comparing its repressive capacity in WT versus $Cry1^{-/-}/Cry2^{-/-}$ MEFs (Figure S1D). Thus, PER2 operates through different mechanisms to represses transcription mediated by CLOCK:BMAL1 or PPARγ.

PER2 Inhibits PPARγ Recruiting to Target Promoters via the Critical S112

To gain insights on the mechanisms of PER2-mediated PPARγ repression, we characterized the PPARγ region recognized by PER2. Different GST-PPARγ fusion proteins were purified and used in GST immunoaffinity assays (Figures 2A and S2A). This analysis identified a region in PPARγ corresponding to the N- terminal A/B domain, harboring a ligand-independent transcriptional activation domain (AF-1) (Tontonoz and Spiegelman, 2008) (Figure 2A). Importantly, PER2 and PPARγ interact in a ligand-independent manner (Figure S2B).

Additional proof of specificity was provided by the lack of interaction between PER2 and PPARα (Figure 2A) and lack of PER2-mediated repression for PPARα and PPARδ-induced transactivation (Figure 2B).

The PPARγ A/B domain contains a serine residue (S112) critical for transcription function (Tontonoz and Spiegelman, 2008). Most studies support a view in which S112 phosphorylation functions as a repressive transcriptional signal (Rangwala et al., 2003). In addition, S112A mutation results in increased PPARγ adipogenic activity *in vitro*, although adipogenesis is not altered *in vivo* (Tontonoz and Spiegelman, 2008). To explore the possibility that S112 may be implicated in the interaction with PER2, we immunoprecipitated proteins from cells transiently expressing Myc-PER2 and PPARγ, or a mutated version of PPARγ with a Ser>Ala mutation at position 112. While PER2 is not affecting the phosphorylation levels of PPARγ (Figure S2C), there is a pronounced reduction of PER2 binding to PPARγ-S112A, compared to the WT protein (Figure 2C). To establish whether S112 phosphorylation may affect PER2 binding, we used increasing amounts of synthetic peptides, either phosphorylated or not at S112, as competitors in GST immunoaffinity assays (Figure 2D). Our results indicate that phosphorylation at S112 increases PER2 binding. To assess whether it is S112 or its phosphorylation that is critical for PER2-mediated repression, we compared the repression by PER2 using PPARγ or

mutants of PPARγ in which S112 has been substituted to mimic a constitutively unphosphorylated (S112A) or phosphorylated (S112D) serine. Lower amounts of PER2 induced repression of S112D but not of the S112A mutant (Figures 2E and S2D). Thus, S112 phosphorylation plays a crucial role in PER2 repression of PPARγ. To explore the mechanisms underlying PER2–mediated repression of PPARγ, we tested whether PER2 affects the recruiting of PPARγ to the PPRE in the *Ap2* gene. Importantly, co-expression of PER2 resulted in a statistically significant reduction in PPARγ recruiting on *Ap2* PPRE, as revealed by chromatin immunoprecipitation (ChIP) assays (Figure 2F). No difference in recruitment was observed with the PPARγ-S112A mutant (Fig 2F). These results reveal a scenario in which PER2-mediated repression is achieved by impairing PPARγ recruitment to target regulatory elements.

A Unique PER2 Domain Directs Interaction with and Repression of PPARγ

The specific interaction of PPARγ with PER2, but not with PER1, indicated the presence in PER2 of a yet uncharacterized functional domain involved in PPARγ repression. To identify this domain, we tested the ability of different PER2 deletions to repress PPARγ-mediated activation (Figure S2E). We identified a C-terminal domain (aa 882-1067), the most divergent region in the three PER proteins (Figure 2G). This region is directly involved in PER2/PPARγ association as demonstrated by MS analysis and co-IP assays (Figure 2H). Its deletion had no effect on protein stability or on subcellular localization (Figure S2F). We identify this region in PER2 as the PPARγ Interacting Domain (PID). We explored whether the PID is involved in PER2-mediated repression of CLOCK:BMAL1-induced activation. While deletion of the PID drastically reduces ability to repress the PPAR-regulated *Ap2* promoter, it has no effect on CLOCK:BMAL1-regulated *Per1* promoter (Figure 2I and S2G).

PER2 Controls Adipocyte Differentiation

PPARγ is known to play a critical role in adipocyte differentiation (Tontonoz and Spiegelman, 2008). Thus, we reasoned that PER2 might be implicated in this control. To test this possibility we used mouse embryo fibroblasts (MEFs) and 3T3-L1 preadipocyte cells.

Per2^-/- and WT MEFs were prepared and then infected with viral vectors expressing GFP, Myc-PER2 or Myc-PER2 PID. Cells were then differentiated in adipocytes in response to an adipogenic induction cocktail (Rosen and MacDougald, 2006). A small proportion of control GFP-expressing WT MEFs differentiated in adipocytes (Figures 3A-E). In contrast, a significantly higher population of *Per2*^-/- MEFs differentiated into adipocytes (Figures 3B and 3E). Also, *Per2*^-/- cells transduced with a PER2 vector showed a degree of differentiation similar to WT cells (Figures 3C and 3E), whereas expression of PER2 PID was not able to rescue the *Per2*^-/- phenotype (Figures 3D and 3E). Consistently, induction of adipocyte specific, PPAR-controlled genes, such as *Adiponectin* and *Ap2* (Rosen and MacDougald, 2006), was significantly higher in differentiated *Per2*^-/- MEFs, compared to WT MEFs (Figure 3F). Importantly, expression of adipocyte genes returned to wild-type levels in PER2-rescued *Per2*^-/- cells, while both *Adiponectin* and *Ap2* expression remained high in PER2 PID-trasduced *Per2*^-/- MEFs (Figure 3F).

Increased adipogenesis was also observed in pre-adipocytes 3T3-L1 cells in which *Per2* expression was knocked-down by RNA interference (Per2b 3T3-L1 in Figures S3A and S3B), as revealed also by the increased *Adiponectin* expression (Figure S3B).

Many genes are regulated in a differentiation-dependent manner during adipogenesis, including *Ppar*γ and C/*ebp*α (Rosen and MacDougald, 2006). Thus, to establish the temporal profile of PER2-PPARγ interaction during 3T3-L1 cells differentiation, we compared the expression levels of *Ppar*γ *C/ebp*α, *Per2* and other clock genes at different times of differentiation (Figure 3G). As previously reported (Soukas et al., 2001), *Ppar*γ and C/*ebp*α expression drastically increases during a 7-days differentiation period, a trend paralleled by *Per2* levels (Figure 3G). *Per2* expression contrasts to other clock genes (*Per1*, *Bmal1* and *Cry1*) whose levels, after an initial increase, remain constant and quite low. Next we analyzed the interaction of PER2 and PPARγ native proteins during the differentiation program. In accordance to the mRNA profile (Figure 3G), PER2 and PPARγ protein levels increased from day 0 to day 6 (Figure 3H and not shown). Levels of co-immunoprecipitated PER2-PPARγ also increased in parallel (Figure 3H). Together, these results indicate that PER2 controls the adipocyte differentiation program through direct regulation of PPARγ.

PER2 Specifies the Adipogenic Gene Expression Program

To further explore the physiological role of PER2-mediated PPARγ repression, we used a whole-genome microarray approach of adipose tissues from *Per2*^{-/-} and WT mice. In WAT from *Per2*^{-/-} animals, expression patterns for 340 out of 28,925 (1.17%) probes changed significantly by 2-fold or more relative to WAT of WT mice. Within this set, 147 individual genes (43%) were upregulated relative to WAT of WT mice (Figure 4C and Table S2). When analyzed for co-occurrence in common biological functions, 98 out of 147 (>65%) upregulated transcripts were found to encode proteins involved in metabolism, response to biotic stimuli or stress, muscle development, ion and electron transport (Figure 4A and Table S2). The majority of these transcripts code for proteins involved in lipid metabolism, and 71% of this subset of genes are known PPARγ targets (Figure 4A and Table S2). This subset of transcripts also includes genes specifically upregulated in WAT of mice treated with PPARγ ligands, such as *Acsm3* (*Mcat*), *Fatp2*, *Pdk4*, *Cpt1b* (Way et al. 2001). Remarkably, the 21 most highly elevated transcripts included the brown adipose tissue (BAT) specific genes *Ucp1*, *Elovl3* and *Cidea* (Seale et al., 2008). In line with the observation that *Per2*^{-/-} mice display no major circadian dysfunction in the adipose tissue (Figure 1I), all circadian genes showed an equivalent expression profile in both genotypes (Table S3).

We then performed a comparative analysis of genes displaying a more than 2-fold change in expression in *Per2*^{-/-} WAT with respect to WT BAT and *Per2*^{-/-} BAT (Figure 4B). This analysis indicated that most transcripts upregulated in *Per2*^{-/-} WAT correspond to genes highly expressed in WT BAT (Figures 4B and 4C). Most transcripts upregulated in *Per2*^{-/-} WAT did not show significant change in *Per2*^{-/-} BAT (Figure 4C and Table S4), indicating a tissue-specific role for PER2 function. Nevertheless, other PPARγ targets were highly expressed in *Per2*^{-/-} BAT (Way et al., 2001), such as *Elovl3*, *Dio2*, *Gys2*, *Hal* and *Rbp7*

(Table S4). This result is consistent with the activation of PPARγ targets by treatment of mice with PPARγ ligands (Way et al., 2001).

Although PPARγ is predominantly expressed in adipocytes, its expression is detected in other tissues (Evans et al., 2004). To further examine the tissue specific action of PER2 on PPARγ we analyzed the expression of BAT specific genes *Ucp1* and *Cidea* in *Per2^-/-* livers. Importantly, both genes displayed negligible differences in expression as compared to WT livers (Figure S4A).

Our microarray analysis also showed that expression of 22 genes in WAT from *Per2^-/-* animals is significantly reduced (2-fold or more) relative to WT mice (Table S2). None of these genes showed significant co-occurrence in common pathways, even using a less stringent cut-off (P<0.001; PPDE<0.95). Lowering the cut-off allowed to group 36 out of 128 genes in biological functions (Table S5).

Notably, 98 out of the 128 genes found (>75%) correspond to genes down-regulated in BAT of WT mice (Table S5). This observation indicates that down-regulation of several genes in the WAT of *Per2^-/-* mice could be due to the overexpression of BAT specific genes. Remarkably, only one of the down-regulated genes, *Bmp7*, has been reported to affect adipogenesis (Tseng et al., 2008). Considering that BMP7 function is to activate a program of brown adipogenesis, its down-regulation does not seem to possibly contribute to the increased expression of BAT genes in the WAT of *Per2^-/-* mice.

RT-PCR analysis confirmed the expression of selective genes for brown fat cells, such as *Ucp1*, *Elovl3* and *Cidea*, in the WAT of *Per2^-/-* mice (Figure 4D). Notably, it has been shown that transgenic mice ectopically expressing brown adipocyte genes in white adipose tissue (Ricquier and Bouillaud, 2000) (Feldmann et al., 2009) (Rossmeisl et al., 2002) (Kopecky et al., 2001) (Leonardsson et al., 2004) display a metabolic phenotype resembling that of *Per2^-/-* mice (Figures 1A-F).

Next we sought to establish whether the altered expression profile reported above was caused by a change in PPARγ function due to the absence of PER2. Thus, we performed ChIP assays from mouse tissues and analyzed whether the recruiting of PPARγ to selected promoters for brown fat cell genes might be altered in *Per2*-null mice. In striking contrast to the situation in WAT from WT mice, we observed specific recruiting of PPARγ to the *Ucp1* PPRE in the WAT from *Per2^-/-* mice (Figure 4E), matching the gene expression profile (Figure 4D). No difference in PPARγ recruitment was observed in BAT from WT versus *Per2^-/-* mice, in keeping with the gene expression profile (Figure 4D). Thus, PER2 seems to dictate the specificity of PPARγ targeting *in vivo* and thereby controls the identity of WAT versus BAT adipocytes.

Based on these findings, we anticipated a lower expression of *Per2* compared to *PPARγ* in BAT from WT mice. Unexpectedly, we found only a slight decrease in *Per2*/*PPARγ* expression ratio in BAT versus WAT from WT animals (12:1 in BAT, 7:1 in WAT). As S112 plays a key role in PER2-mediated PPARγ repression (Figure 2), we considered the possibility that PER2 tissue specific action may relate to S112 phosphorylation degree in WAT versus BAT. To test this hypothesis, we performed an immunoblot analysis in white

and brown adipose tissue from WT mice using both a specific PPARγ antibody and an antibody recognizing endogenous levels of PPARγ only when phosphorylated at S112. Consistently, S112 phosphorylation levels were markedly reduced by ~65% in BAT compared to WAT (Figure S4C).

To gain further understanding in the altered lipid metabolism of $Per2^{-/-}$ mice, we classified the highly expressed transcripts in $Per2^{-/-}$ WAT according to their cooccurrence in common metabolic pathways (Figure 4F).

This subset includes several genes coding for mitochondrial proteins whose enzymatic activity is directly involved in fatty acid β-oxidation, such as the Acyl-CoA dehydrogenases for short, medium, long and very-long chain fatty acids (*Acads*, *Acadm*, *Acadl*, *Acadvl*) and the 3-ketoacyl-CoA thiolase (*Hadha* and *Hadhb*), which catalyzes the last three steps of mitochondrial β-oxidation of long chain fatty acids (Hashimoto, 1999). Deletion of *Per2* also resulted in overexpression of the *Cpt1b* gene, which encodes for a member of the carnitine/choline acetyltransferase family, the rate-controlling enzyme of the long-chain fatty acid β-oxidation. This subset of transcripts also includes genes coding for enzymes involved in amino acid degradation and Tricarboxylic Acid (TCA) cycle that can produce metabolites for the uncoupled oxidative phosphorylation pathway (Figure 4F). In addition, *Ucp1*, the product of which is involved in the uncoupling of oxidative phosphorylation (Ricquier and Bouillaud, 2000), and *Cox7a1* and *Cox8b*, coding for enzymes of the Cytochrome c oxidase complex IV (Kadenbach et al., 2000) were also highly overexpressed in WAT from $Per2^{-/-}$ mice (Figure 4F). Notably, an increased activation of these enzymes has been shown both *in vitro* and *in vivo* in response to PPARγ agonist treatment, at least under some conditions (Fukui et al., 2000) (Wilson-Fritch et al., 2004).

To further support the array data, we determined the enzymatic activity of cytochome oxidase complex IV and CPT1 in mitochondria preparation from WAT of WT and $Per2^{-/-}$ mice. Consistent with the gene expression analysis, the activity of both enzymatic complexes showed a significant increase in mutant animals when compared to WT littermates (Figures 4G and 4H). These analyses reveal that the metabolic phenotype of the $Per2^{-/-}$ animals is likely to result from altered lipid metabolism in WAT.

Adipocyte-Autonomous Effect of PER2

In order to establish that the effect of PER2 on gene transcription is caused by its function intrinsic to adipocytes, we decided to knock-down its expression by RNA interference. We analyzed the expression of the adipogenic marker *Adiponectin* and the BAT-specific genes *Ucp1* and *Cidea* in pre-adipocyte 3T3-L1 cells. A 50% decrease in PER2 levels induced by the knock-down (Figure S3A), resulted in a significant increase in the expression of *Adiponectin, Cidea* and *Ucp1*, while *Bmal1* expression is unaffected (Figure S3B). Analogous results were obtained in *Per2*-deficient MEFs (Figure S3C). These findings demonstrate that PER2 is critical in the control of adipogenic and BAT-specific genes in a system where adipocyte cell control is autonomous of other cell types.

PER2 Regulates Lipid Metabolism in White Adipose Tissue

To test whether PER2 is implicated in controlling lipid metabolism in WAT, we conducted an unbiased lipidomic analysis on $Per2^{-/-}$ and WT mice. These studies revealed a marked reduction in total TAG levels (Figure 5A) in $Per2$-null mice, while the total NEFA levels remain comparable to WT (Figure 5B). Considering the overexpression of fatty acid-binding protein $Fabp3$ in $Per2^{-/-}$ WAT (Figure 4F), we expected higher levels of FA in $Per2^{-/-}$ WAT. In fact, FABP3 is required for shuttling FA through the cytosol, and $Fabp3$-null mutation in isolated soleus muscle results in FA transport reduction (Binas et al., 2003). However, an increased FA transport could be compensated by a higher oxidative capability, as suggested by the expression of several genes involved in FA oxidation increases in $Per2^{-/-}$ WAT (Figure 4F).

A detailed, comparative FA analysis by HPLC-MS between WT and $Per2$-null WAT revealed significant elevation in levels of saturated (SFA) and monosaturated (MUFA) very long chain fatty acids (VLCFAs) (Figure 5C). No relevant differences were observed for polysaturated (PUFA) VLCFAs and long-chain fatty acids (LCFAs) (Figures 5C and 5D). SFA and MUFA VLCFAs are biosynthetic products of a fatty acid elongase coded by the brown fat PPARγ target gene, $Elovl3$, the transcript of which is induced in the WAT of $Per2$-null mice (Figure 4D). The enzyme ELOVL3 is implicated in the synthesis of VLCFAs (SFA and MUFA) to replenish their intracellular pools when fatty acid turnover rate is high due to an increased FA oxidation (Westerberg et al., 2006).

As both genomic and lipidomic analysis support a function for PER2 in the regulation of FA oxidation in WAT, we further analyzed FA oxidation in adipocytes by measuring the conversion of [U-^{14}C]-palmitate into $^{14}CO_2$ (Wang et al., 2003). Consistent with increased oxidation $Per2$-null adipocytes released twice as much $^{14}CO_2$ than WT adipocytes over a 2h period (Figure 5E). We then evaluated fatty acids oxidation in WAT sections using the 2,3,5-triphenyltetrazolium chloride (TTC) method. In agreement with $^{14}CO_2$ measurements, quantification by TTC staining intensity revealed a 2-fold increase in fatty acids oxidation in $Per2^{-/-}$ mice (Figure 5F).

We further investigated whether the impact of PER2 on WAT may result in altered adipocyte morphology. Adipocytes from $Per2^{-/-}$ mice were significantly smaller than WT, as determined by histological analysis (Figures 5G and 5H). The WAT of $Per2$-null mice was almost completely deprived of adipocytes larger than 150 micrometers (Figure 5I). Thus, PER2 appears to control lipid metabolism by direct regulation of PPARγ.

Circadian-related effect of PER2 on PPARγ target genes

Although the expression of BAT specific genes in $Per2^{-/-}$ WAT indicates a circadian-independent function for PER2 in this tissue, both $Per2$ and $Ppar\gamma$ oscillate in WAT (Yang et al., 2007). Therefore we analyzed if $Per2$ deletion could produce differences in circadian expression of PPARγ regulated genes in WAT. As reported (Yang et al., 2007), circadian expression profile analysis in WAT shows a synchronous oscillation of PPARγ targets $Fabp4$ and $Adiponectin$, with peaks around ZT14 (Figure S6A). Remarkably, while $Per2$

deletion did not alter circadian expression of CLOCK:BMAL1 targets (Figure 1), it changed both phase and amplitude of *Pparγ* targets in WAT (Figure S6A).

Our results underscore the role of S112 in PER2-mediated PPARγ repression (Figure 2). Since S112 phosphorylation is significantly reduced in BAT as compared to WAT (Figure S4C), we reasoned that information on the contribution of PER2 on circadian PPARγ regulation may came from a circadian analysis of PPARγ targets in BAT (Figure S6B). Notably, this analysis revealed a remarkable similarity of *Adiponectin* and *Fabp4* circadian profile in WT BAT and *Per2^-/-* WAT (Figure S6B). In addition, ablation of *Per2* produced negligible effects on circadian expression of PPARγ regulated genes in BAT (Figure S6B). Overall, these data support the scenario of a PER2 tissue specific action on PPARγ mediated by S112 phosphorylation.

DISCUSSION

PPARγ was initially characterized as master regulator of the differentiation of fibroblasts-like mesenchymal stem cells into adipocytes, the process known as adipogenesis (Evans et al., 2004). In addition, its further implication in widespread diseases, as diabetes, inflammation and cancer, places PPARγ in a strategic position for the development of drugs (Tontonoz and Spiegelman, 2008).

Here we report that PER2 forms a complex with PPARγ and regulates its function. An intriguing observation made 16 years ago indicated that a PPARγ lacking the first 120 aa gained in transcriptional potency and induced adipogenesis more efficiently (Tontonoz et al., 1994). This was unexpected as the N-terminal region of most nuclear receptors contains the activation domain (Tontonoz and Spiegelman, 2008). In PPARγ however, this region appears to operate as an intermolecular repressor domain. Further studies established the critical role of S112 for this inhibitory function (Compe et al., 2005) (Rangwala et al., 2003). We demonstrate that PER2 represses PPARγ by interacting with the N-terminal domain, and S112 is critical for this effect (Figures 1 and 2).

Relief of PER2-mediated PPARγ repression in mice in which *Per2* is fully ablated (*Per2^-/-*) results in profound alterations in adiposity and systemic lipid metabolism (Figures 1 and 5). Remarkably, another line of *Per2* mutant mice carrying a deletion of the PAS domain (*Per2^m/m* mice; (Zheng et al., 1999)) resulted in confusing results, showing either normal (Feillet et al., 2006) or decreased weight (Yang et al., 2009), very likely because the *Per2^Brdm1* allele in *Per2^m/m* mice does not act as a real loss-of-function allele (Shearman et al., 2000). In contrast with *Per2^-/-* animals, *Per2^m/m* mice also presented defects in food anticipatory activity (Storch and Weitz, 2009).

PER2 exerts its repressive action on PPARγ by blocking its recruiting to target promoters (Figures 2F and 4E), a mechanism that is conceptually different from the repression that PER2:CRY exert on CLOCK:BMAL1 (Bae et al., 2001). Indeed, while CRY proteins enhance PER2 repressive action on CLOCK:BMAL1, they have no effect on PPARγ (Figure S1C). These differences highlight the presence of two independent pathways of PER2 function, which utilize fundamentally different mechanisms and specificity. Indeed,

PER1 does not interact with nor represses PPARγ (Figures 1K and M). All PERs are highly structurally related, but differ in the C-terminal domain (Hirayama and Sassone-Corsi, 2005). We have identified the PID that is located in the divergent C-terminal of PER2 (Figure 2G). Our results reveal a circadian-independent repressive function of PER2 specific for PPARγ: a PID-deleted PER2 is still able to efficiently repress CLOCK:BMAL1 (Figure 2I). In support to this concept, circadian gene expression is basically unaltered in the SCN (Bae et al., 2001) and in WAT (Figure 1I) of *Per2*-null mice. In marked contrast, *Per2* ablation in WAT results in circadian changes of PPARγ target genes (Figure S6A).

Consistent with a PER2-mediated repression of PPARγ, both ablation and knock-down of *Per2* results in increased activation of adipogenic genes, as well as brown adipogenic markers (Figures 3 and S3)

Despite the repression effect of PER2 on *in vitro* adipogenesis, *Per2* deletion does not increase adiposity *in vivo* (Figure 1B). Importantly, several mice mutants for transcriptional regulators affecting adipocyte differentiation display differences between *in vitro* and *in vivo* adipogenesis (Leonardsson et al., 2004) (Rangwala et al., 2003), indicating that several factors account for the divergence between cultured cells and adipose tissue. This notion is supported by distinct transcriptional profiles of adipogenesis *in vivo* and *in vitro* (Soukas et al., 2001).

Comparative gene expression profiles support a PER2 repressive action on PPARγ targets also *in vivo* (Figure 4). In addition, both gene profiling and mitochondrial protein activity assays point to specific pathways of metabolic control, specifically β-oxidation, fatty acid synthesis and elongation, and TCA synthesis (Figure 4F).

Although PPARγ is expressed in tissues other than WAT (Evans et al., 2004), *Per2* effect on PPARγ activity seems to be tissue specific. Indeed, *Per2* deletion directs the expression of BAT specific genes in WAT (Figure 4), but not in BAT and liver (Figures S4A and C). In addition, there are significant differences in TGA contents in WAT (Figure 5A), but not in BAT or liver of *Per2*^{−/−} mice (Figure S5). Overall, our data support a scenario in which PER2 operates as a natural repressor of PPARγin a WAT–specific manner (Figure 6B). This tissue specificity is further supported by the prominent effect of *Per2* deletion on the expression of PPAR target genes and oscillation in WAT than in BAT (Figures 4 and S6). Importantly, we identified S112 phosphorylation as critical element in the regulation of PER2-mediated tissue specific action. Indeed, S112 phosphorylation levels in BAT are strikingly reduced as compared to WAT (Figure S4C), in keeping with a low *Per2* repression activity in BAT. Since PER2 appears to interact with other nuclear receptors (Schmutz et al. 2010), we hypothesize that PER2 may regulate multiple pathways in a tissue specific manner (Figure 6C). The physiological implications of our findings are multiple and indicate the potential for promising pharmacological intervention.

EXPERIMENTAL PROCEDURES

Animals

Per2⁻/⁻ mice were kindly provided by S. Reppert (Bae et al., 2001). Animals were housed under 12 hr light/12 hr dark (LD) cycles. For blood and tissue TGA and free FFA, mice were fasted for 3 hrs before collect samples. All protocols using animals were approved by the IACUC of UC, Irvine.

Plasmids

Vectors expressing PPARγ2, Flag-PPARγ2, Flag-PPARγ1 and Flag-S112A PPARγ were kindly provided by Bruce Spiegelman. The *Per2* coding sequence was cloned in pCS+MT2. To delete the PPARγ Interacting Domain (PID), the *Per2* coding sequence was cut with Xcm I to remove the C-terminal domain of PER2 from aa 882 to the stop codon (PER2 C). The *Per2* sequence equivalent to a protein segment from aa 1067 to the stop codon was amplified by PCR and introduced in the PER2 C vector.

Cell culture

3T3-L1 cells and NIH 3T3 cells were maintained in DMEM supplemented with 10% FBS and antibiotics. JEG3 cells were grown in BME supplemented with 10% FBS and antibiotics. MEFs were generated from WT or *Per2⁻/⁻* homozygous sibling mice and cultured in DMEM supplemented with 10% FBS.

Protein extracts, immunoprecipitation and western analyses

Cells were lysed in L buffer (150mM NaCl, 5mM EDTA, 0.5%NP-40, 50 mM Tris-HCl (pH 7.8), protease inhibitors) for co-IP. Protein samples were immunoblotted with α-Myc(Millipore), α-Flag (Sigma), α-PPARγ and α-S112 PPARγ (Cell Signaling), and α-PER2 (Siepka et al., 2007).

qRT-PCR

Each quantitative real-time RT-PCR was performed using the Chromo4 real time detection system (BIO-RAD).

GST Pulldown Assays

GST-fused recombinant proteins were expressed in *E. coli* BL21. Recombinant proteins were purified by CelLytic B Reagent (Sigma) according to the manufacturer's protocol. ^{35}S-meth-labeled proteins were made *in vitro* using the TNT-T7 quick-coupled transcription-translation system (Promega). A scheme of the deleted GST-PPARγ2 fusion proteins is shown in Figure 2.

Chromatin immunoprecipitation (ChIP) analysis

ChIP assays were performed as described (Doi et al., 2006), with minor modification. For ChIP assay from WAT and BAT, tissues were crosslinked in PBS; 1% formaldehyde and homogenated in buffer A (15mM Hepe pH 7.5; 60mM KCl; 0.3M Sucrose; 0.5mM DTT) to prepare nuclei.

FA Oxidation Assays

Isolated adipocytes were mixed with 300μl of 2% FFA-free BSA-KRB containing 40μCi/ml [14C]palmitic acid (Perkin Elmer Life Sciences). After washing, adipocytes were mixed with 500 μl of 2% FFA-free BSA-KRB and incubated in 50 ml tube for 2 hrs at 37C. The $^{14}CO_2$ produced was released by injection of 0.5 ml of 10N H_2SO_4 for β-counting measurements.

Mass Spectrometry

PER2 C-terminal domain from aa882 to stop fused with a Flag epitope and a Flag-GFP were transfected in JEG3 cells for immunoprecipitation analysis. Co-IP proteins analysed by MALDI mass spectrometry as described in online method.

Lipidomic Analyses

For lipid identification and quantification we used an 1100-LC system coupled to a 1946A-MS detector (Agilent Technologies, Inc., Santa Clara, CA) equipped with an electrospray ionization (ESI) interface.

Mitochondria Preparation, complex IV and CPT1 Activity Assay

Epididymal WAT was homogenized in buffer A (MOPS 1X; 250 mM Sucrose; 0.25 mM reduced Glutathione; 2% FA-free BSA) and centrifuged 15 min 600xg at 4°C. After removal of upper fat layer, supernatant was collected in new tubes and centrifuged 15 min 8000xg at 4°C. Pellet was resuspended in 1 ml of buffer A and centrifuged 15 min 800xg at 4°C. Mitochondria were resuspended in 100 μl of KCl 150 mM and protein concentration was determined by BCA assay. Complex IV and CPT1 Activity were assessed as described in supplementary methods.

Target Preparation/Processing for GeneChip® *WT Sense Target Analysis*

All the information on microarray including the raw data is available online at GEO website (www.ncbi.nlm.nih.gov/geo/query/acc.cgi?token=xxorfsmsismusro&acc=GSE20165).

Supplementary Material

Refer to Web version on PubMed Central for supplementary material.

Acknowledgments

REFERENCES

Akhtar RA, Reddy AB, Maywood ES, Clayton JD, King VM, Smith AG, Gant TW, Hastings MH, Kyriacou CP. Circadian cycling of the mouse liver transcriptome, as revealed by cDNA microarray, is driven by the suprachiasmatic nucleus. Curr Biol. 2002; 12:540–550. [PubMed: 11937022]

Bae K, Jin X, Maywood ES, Hastings MH, Reppert SM, Weaver DR. Differential functions of mPer1, mPer2, and mPer3 in the SCN circadian clock. Neuron. 2001; 30:525–536. [PubMed: 11395012]

Binas B, Han XX, Erol E, Luiken JJ, Glatz JF, Dyck DJ, Motazavi R, Adihetty PJ, Hood DA, Bonen A. A null mutation in H-FABP only partially inhibits skeletal muscle fatty acid metabolism. American journal of physiology. 2003; 285:E481–489. [PubMed: 12900378]

Compe E, Drane P, Laurent C, Diderich K, Braun C, Hoeijmakers JH, Egly JM. Dysregulation of the peroxisome proliferator-activated receptor target genes by XPD mutations. Molecular and cellular biology. 2005; 25:6065–6076. [PubMed: 15988019]

Duffield GE, Best JD, Meurers BH, Bittner A, Loros JJ, Dunlap JC. Circadian programs of transcriptional activation, signaling, and protein turnover revealed by microarray analysis of mammalian cells. Curr Biol. 2002; 12:551–557. [PubMed: 11937023]

Eckel-Mahan K, Sassone-Corsi P. Metabolism control by the circadian clock and vice versa. Nat Struct Mol Biol. 2009; 16:462–467. [PubMed: 19421159]

Evans RM, Barish GD, Wang YX. PPARs and the complex journey to obesity. Nat Med. 2004; 10:355–361. [PubMed: 15057233]

Feillet CA, Ripperger JA, Magnone MC, Dulloo A, Albrecht U, Challet E. Lack of food anticipation in Per2 mutant mice. Curr Biol. 2006; 16:2016–2022. [PubMed: 17055980]

Feldmann HM, Golozoubova V, Cannon B, Nedergaard J. UCP1 ablation induces obesity and abolishes diet-induced thermogenesis in mice exempt from thermal stress by living at thermoneutrality. Cell Metab. 2009; 9:203–209. [PubMed: 19187776]

Field MD, Maywood ES, O'Brien JA, Weaver DR, Reppert SM, Hastings MH. Analysis of clock proteins in mouse SCN demonstrates phylogenetic divergence of the circadian clockwork and resetting mechanisms. Neuron. 2000; 25:437–447. [PubMed: 10719897]

Fukui Y, Masui S, Osada S, Umesono K, Motojima K. A new thiazolidinedione, NC-2100, which is a weak PPAR-gamma activator, exhibits potent antidiabetic effects and induces uncoupling protein 1 in white adipose tissue of KKAy obese mice. Diabetes. 2000; 49:759–767. [PubMed: 10905484]

Hashimoto T. Peroxisomal beta-oxidation enzymes. Neurochem Res. 1999; 24:551–563. [PubMed: 10227687]

Hirayama J, Sassone-Corsi P. Structural and functional features of transcription factors controlling the circadian clock. Curr Opin Genet Dev. 2005; 15:548–556. [PubMed: 16095901]

Kadenbach B, Huttemann M, Arnold S, Lee I, Bender E. Mitochondrial energy metabolism is regulated via nuclear-coded subunits of cytochrome c oxidase. Free Radic Biol Med. 2000; 29:211–221. [PubMed: 11035249]

King DP, Takahashi JS. Molecular genetics of circadian rhythms in mammals. Annu Rev Neurosci. 2000; 23:713–742. [PubMed: 10845079]

Kopecky J, Rossmeisl M, Flachs P, Bardova K, Brauner P. Mitochondrial uncoupling and lipid metabolism in adipocytes. Biochem Soc Trans. 2001; 29:791–797. [PubMed: 11709076]

Lee C, Weaver DR, Reppert SM. Direct association between mouse PERIOD and CKIepsilon is critical for a functioning circadian clock. Molecular and cellular biology. 2004; 24:584–594. [PubMed: 14701732]

Lehmann JM, Moore LB, Smith-Oliver TA, Wilkison WO, Willson TM, Kliewer SA. An antidiabetic thiazolidinedione is a high affinity ligand for peroxisome proliferator-activated receptor gamma (PPAR gamma). J Biol Chem. 1995; 270:12953–12956. [PubMed: 7768881]

Lehrke M, Lazar MA. The many faces of PPARgamma. Cell. 2005; 123:993–999. [PubMed: 16360030]

Leonardsson G, Steel JH, Christian M, Pocock V, Milligan S, Bell J, So PW, Medina-Gomez G, Vidal-Puig A, White R, Parker MG. Nuclear receptor corepressor RIP140 regulates fat accumulation. Proceedings of the National Academy of Sciences of the United States of America. 2004; 101:8437–8442. [PubMed: 15155905]

Panda S, Antoch MP, Miller BH, Su AI, Schook AB, Straume M, Schultz PG, Kay SA, Takahashi JS, Hogenesch JB. Coordinated transcription of key pathways in the mouse by the circadian clock. Cell. 2002; 109:307–320. [PubMed: 12015981]

Rangwala SM, Rhoades B, Shapiro JS, Rich AS, Kim JK, Shulman GI, Kaestner KH, Lazar MA. Genetic modulation of PPARgamma phosphorylation regulates insulin sensitivity. Dev Cell. 2003; 5:657–663. [PubMed: 14536066]

Reppert SM, Weaver DR. Coordination of circadian timing in mammals. Nature. 2002; 418:935–941. [PubMed: 12198538]

Ricquier D, Bouillaud F. Mitochondrial uncoupling proteins: from mitochondria to the regulation of energy balance. J Physiol. 2000; 529(Pt 1):3–10. [PubMed: 11080246]

Rosen ED, MacDougald OA. Adipocyte differentiation from the inside out. Nat Rev Mol Cell Biol. 2006; 7:885–896. [PubMed: 17139329]

Rossmeisl M, Barbatelli G, Flachs P, Brauner P, Zingaretti MC, Marelli M, Janovska P, Horakova M, Syrovy I, Cinti S, Kopecky J. Expression of the uncoupling protein 1 from the aP2 gene promoter stimulates mitochondrial biogenesis in unilocular adipocytes in vivo. Eur J Biochem. 2002; 269:19–28. [PubMed: 11784294]

Sahar S, Sassone-Corsi P. Metabolism and cancer: the circadian clock connection. Nature Reviews Cancer. 2009; 9:886–896.

Schibler U, Sassone-Corsi P. A web of circadian pacemakers. Cell. 2002; 111:919–922. [PubMed: 12507418]

Schmutz I, Ripperger JA, Baeriswyl-Aebischer S, Albrecht U. The mammalian clock component PERIOD2 coordinates circadian output by interaction with nuclear receptors. Genes & development. 24:345–357. [PubMed: 20159955]

Schwarz EJ, Reginato MJ, Shao D, Krakow SL, Lazar MA. Retinoic acid blocks adipogenesis by inhibiting C/EBPbeta-mediated transcription. Molecular and cellular biology. 1997; 17:1552–1561. [PubMed: 9032283]

Seale P, Bjork B, Yang W, Kajimura S, Chin S, Kuang S, Scime A, Devarakonda S, Conroe HM, Erdjument-Bromage H, Tempst P, Rudnicki MA, Beier DR, Spiegelman BM. PRDM16 controls a brown fat/skeletal muscle switch. Nature. 2008; 454:961–967. [PubMed: 18719582]

Shearman LP, Sriram S, Weaver DR, Maywood ES, Chaves I, Zheng B, Kume K, Lee CC, van der Horst GT, Hastings MH, Reppert SM. Interacting molecular loops in the mammalian circadian clock. Science. 2000; 288:1013–1019. [PubMed: 10807566]

Siepka SM, Yoo SH, Park J, Song W, Kumar V, Hu Y, Lee C, Takahashi JS. Circadian mutant Overtime reveals F-box protein FBXL3 regulation of cryptochrome and period gene expression. Cell. 2007; 129:1011–1023. [PubMed: 17462724]

Soukas A, Socci ND, Saatkamp BD, Novelli S, Friedman JM. Distinct transcriptional profiles of adipogenesis in vivo and in vitro. J Biol Chem. 2001; 276:34167–34174. [PubMed: 11445576]

Storch KF, Weitz CJ. Daily rhythms of food-anticipatory behavioral activity do not require the known circadian clock. Proceedings of the National Academy of Sciences of the United States of America. 2009; 106:6808–6813. [PubMed: 19366674]

Tontonoz P, Hu E, Spiegelman BM. Stimulation of adipogenesis in fibroblasts by PPAR gamma 2, a lipid-activated transcription factor. Cell. 1994; 79:1147–1156. [PubMed: 8001151]

Tontonoz P, Spiegelman BM. Fat and beyond: the diverse biology of PPARg. Annu Rev Biochem. 2008; 77:289–312. [PubMed: 18518822]

Tseng YH, Kokkotou E, Schulz TJ, Huang TL, Winnay JN, Taniguchi CM, Tran TT, Suzuki R, Espinoza DO, Yamamoto Y, Ahrens MJ, Dudley AT, Norris AW, Kulkarni RN, Kahn CR. New role of bone morphogenetic protein 7 in brown adipogenesis and energy expenditure. Nature. 2008; 454:1000–1004. [PubMed: 18719589]

Wang S, Subramaniam A, Cawthorne MA, Clapham JC. Increased fatty acid oxidation in transgenic mice overexpressing UCP3 in skeletal muscle. Diabetes Obes Metab. 2003; 5:295–301. [PubMed: 12940866]

Way JM, Harrington WW, Brown KK, Gottschalk WK, Sundseth SS, Mansfield TA, Ramachandran RK, Willson TM, Kliewer SA. Comprehensive messenger ribonucleic acid profiling reveals that peroxisome proliferator-activated receptor gamma activation has coordinate effects on gene expression in multiple insulin-sensitive tissues. Endocrinology. 2001; 142:1269–1277. [PubMed: 11181544]

Westerberg R, Mansson JE, Golozoubova V, Shabalina IG, Backlund EC, Tvrdik P, Retterstol K, Capecchi MR, Jacobsson A. ELOVL3 is an important component for early onset of lipid recruitment in brown adipose tissue. J Biol Chem. 2006; 281:4958–4968. [PubMed: 16326704]

Wijnen H, Young MW. Interplay of circadian clocks and metabolic rhythms. Annu Rev Genet. 2006; 40:409–448. [PubMed: 17094740]

Wilson-Fritch L, Nicoloro S, Chouinard M, Lazar MA, Chui PC, Leszyk J, Straubhaar J, Czech MP, Corvera S. Mitochondrial remodeling in adipose tissue associated with obesity and treatment with rosiglitazone. J Clin Invest. 2004; 114:1281–1289. [PubMed: 15520860]

Yang S, Liu A, Weidenhammer A, Cooksey RC, McClain D, Kim MK, Aguilera G, Abel ED, Chung JH. The role of mPer2 clock gene in glucocorticoid and feeding rhythms. Endocrinology. 2009; 150:2153–2160. [PubMed: 19179447]

Yang X, Lamia KA, Evans RM. Nuclear receptors, metabolism, and the circadian clock. Cold Spring Harbor symposia on quantitative biology. 2007; 72:387–394.

Young MW, Kay SA. Time zones: a comparative genetics of circadian clocks. Nat Rev Genet. 2001; 2:702–715. [PubMed: 11533719]

Zheng B, Larkin DW, Albrecht U, Sun ZS, Sage M, Eichele G, Lee CC, Bradley A. The mPer2 gene encodes a functional component of the mammalian circadian clock. Nature. 1999; 400:169–173. [PubMed: 10408444]

Zylka MJ, Shearman LP, Weaver DR, Reppert SM. Three period homologs in mammals: differential light responses in the suprachiasmatic circadian clock and oscillating transcripts outside of brain. Neuron. 1998; 20:1103–1110. [PubMed: 9655499]
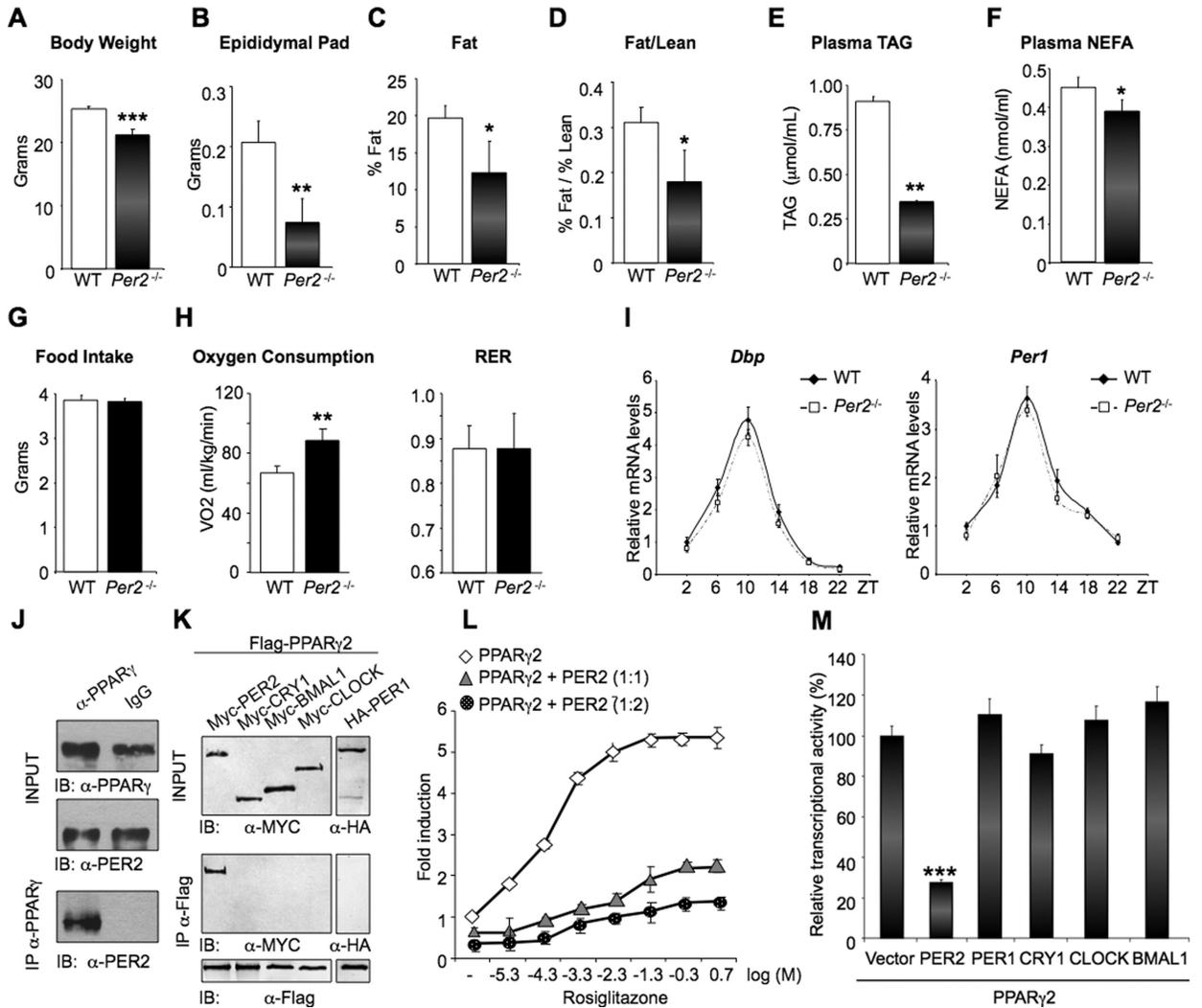
Fig 1. Specific interaction and repression of PER2 on PPARγ

(A) and (B) body and epididymal pad weight of *Per2*$^{-/-}$ and WT mice. (**P<0.01 and ***P<0.001). (C) and (D) body composition of fat (C) and fat/lean ratio (D) analyzed by MRI (*P<0.05). (E) and (F) Triglyceride (TAG) and non-esterified fatty acid (NEFA) in *Per2*$^{-/-}$ and WT plasma samples. (*P<0.05 and **P<0.01). (G) Food pellet grams consumed per day. (H) Oxygen consumption and Respiratory Exchange Ratio (RER) of animals monitored for 48 hrs on normal diet. (**P<0.01). (I) qRT-PCR analysis of *Dbp* and *Per1* in WAT at the indicated Zeitgeber Time (ZT). (J) PPARγ was immunoprecipitated from mouse WAT. Total lysates (INPUT) and IP samples were analyzed by IB with PER2 antibody. (K) Flag-PPARγ was immunoprecipitated from JEG-3 cells co-transfected with the indicated tagged CLOCK proteins. Total lysates (INPUT) and IP samples were analyzed by IB with the indicated antibodies. (L) Effect of different concentrations of rosiglitazone (expressed as Log [μM]) on a PPAR-driven reporter (*PPRE3-TK-luc*) in the presence of 50 ng PPARγ (diamonds) or 50 ng PPARγ and 50 ng (triangles) or 100 ng (circles) of PER2. (M) Comparison between the effect of PER2 and CLOCK used in (I) on PPARγ-mediated transcription in the presence of 10μM rosiglitazone. (***P<0.001).
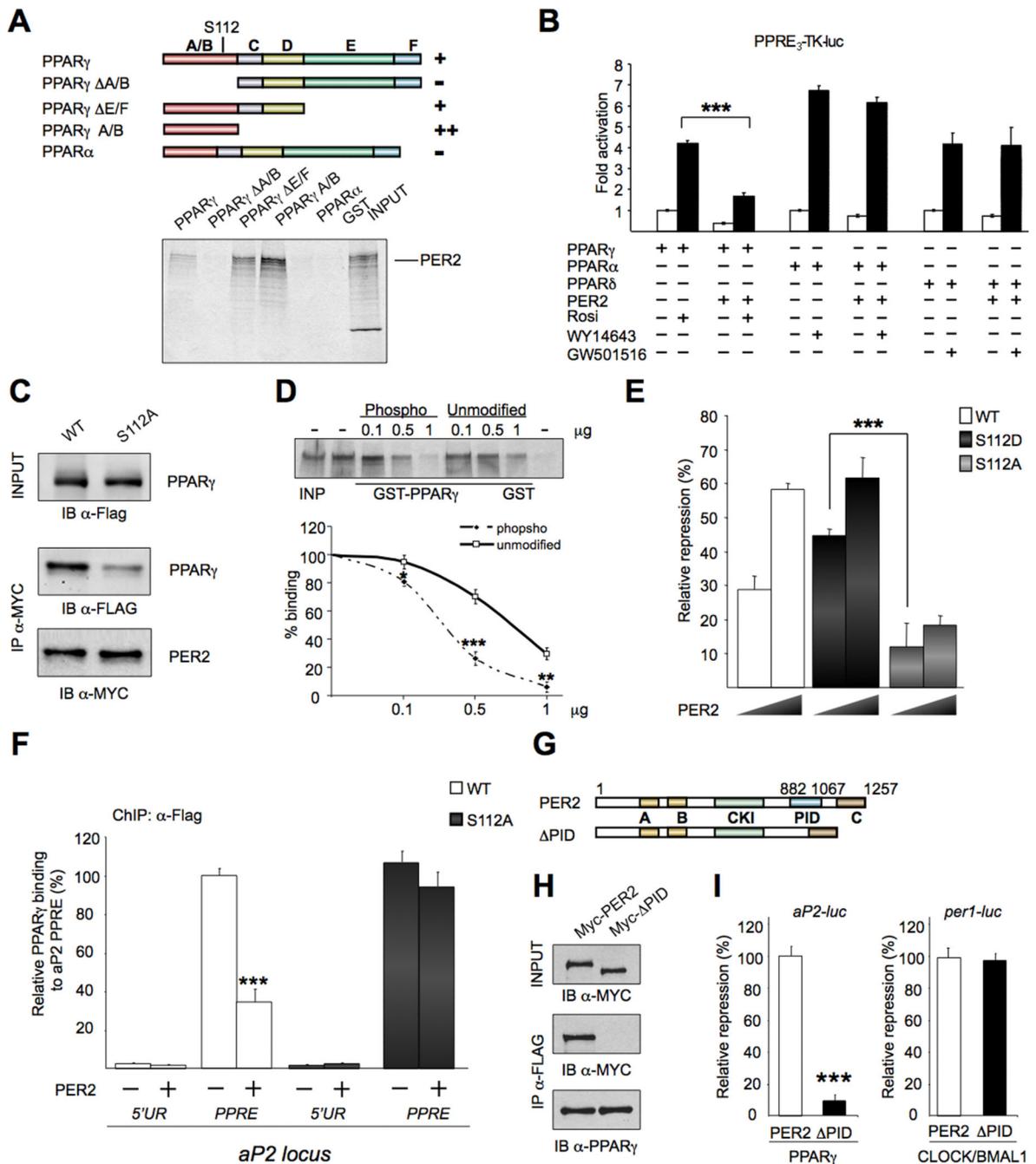
Fig 2. PER2 and PPARγ interacting domains
(A) Schematic representation of PPARγ domains. (A/B) AF1 domain, (C) DNA binding domain, (D) flexible hinge region, (E) ligand binding domain, (F) AF2 domain. GST fusions proteins binding (+) or no binding (-) to ^{35S}PER2 is shown. An example of GST pull-down is shown. (B) Transcriptional activity of *PPRE3-TK-luc* in the presence of PPARs isoforms and PER2 (+) or vector (-). (***$P<0.001$). (C) PER2 interaction with PPARγ is reduced by the S112A mutation. Top panel, IB of total cell lysates (INPUT) with α-Flag antibody. Middle panel, IB of precipitated Myc-PER2 and co-precipitated Flag-PPARγ or Flag-

PPARγ S112A mutant. Bottom, immunoblot analysis of precipitated Myc-PER2. (D) GST immunoaffinity experiments using different concentration (0.1, 0.5, and 1 μg) of an unphosphorylated synthetic peptide (Unmodified) or its phosphorylated serine (PPARγ S112) version (Phospho) as competitors in binding reactions. (*$P<0.05$, **$P<0.01$ and ***$P<0.001$). (E) Repression by PER2 of activated PPARγ (WT) and PPARγ S112A (S112A) or (S112D) mutants. (***$P<0.001$). (F) ChIP assay on 3T3-L1 transiently expressing Flag-PPARγ wild-type (WT) or Flag-PPARγ S112A mutant (S112) and vector (-) or Myc-PER2 (+) (see experimental procedure). Immunoprecipitated DNA was analyzed by qPCR with specific primers for the *Ap2* locus region flanking the PPAR Responsive Element (PPRE) or an upstream region (5′UR) (***$P<0.001$). (G) Schematic representation of PER2 domains (A) PASA, (B) PASB, (CKI) Casein Kinase Interacting, (PID) PPARγ Interacting Domain, (C) CRY interacting domain. Lower scheme, PER2 deleted in PID used in (H) and (I). (H) Flag-PPARγ immunoprecipitated from lysates of JEG3 cells transiently expressing Myc-PER2 or Myc-PER2 without PID (Myc- PID). Total lysates (INPUT) and IP samples analyzed by WB with indicated antibodies. (I) Repression of PER2 and PER2 PID (PID) on the activity of PPARγ- or CLOCK:BMAL1-dependent promoter targets (*Ap2-luc* or *Per1-luc*, respectively) (***$P<0.001$).
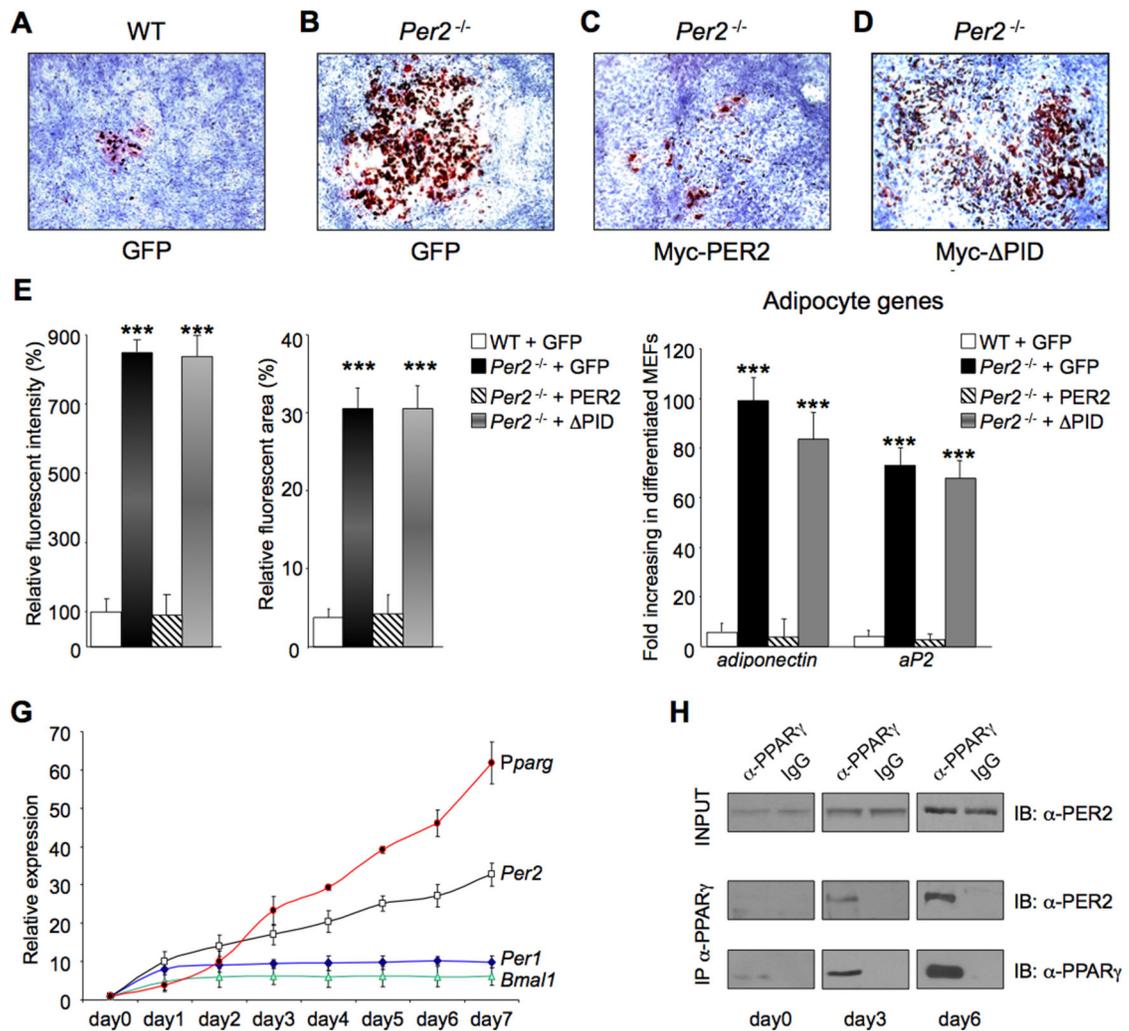
Fig 3. Deletion of *Per2* affects adipocyte differentiation

WT and *Per2^-/-* MEF cells expressing retroviral Myc-GFP (A and B), Myc-PER2 (C), or MycPER2 PID (Myc- PID) (D) were stained with Oil Red O after inducing adipocyte differentiation. (E) The degree of differentiation analyzed by the fluorescent intensity of the Oil Red O staining. (***$P<0.001$). (F) MEFs in (A-D) were analyzed for expression of the adipocyte markers, *Adiponectin* and *Ap2* by qRT-PCR. Values presented as fold induction of mRNA in differentiated versus undifferentiated MEF cells. (***$P<0.001$). (G) qRT-PCR analysis of *Pparg*, *Per2*, *Per1* and *Bmal1* from RNA samples prepared from 3T3-L1 cells collected before (day0) and after (day1-day7) adding the differentiation medium. (H) PPARγ was immunoprecipitated from lysates of 3T3-L1 cells collected at day0, day3 and day6 after adding differentiation media. Top, IB analysis of total cell lysates (INPUT) with an α-PER2 antibody. Middle, IB analysis of co-precipitated PER2. Bottom, IB analysis of immunoprecipitated PPARγ
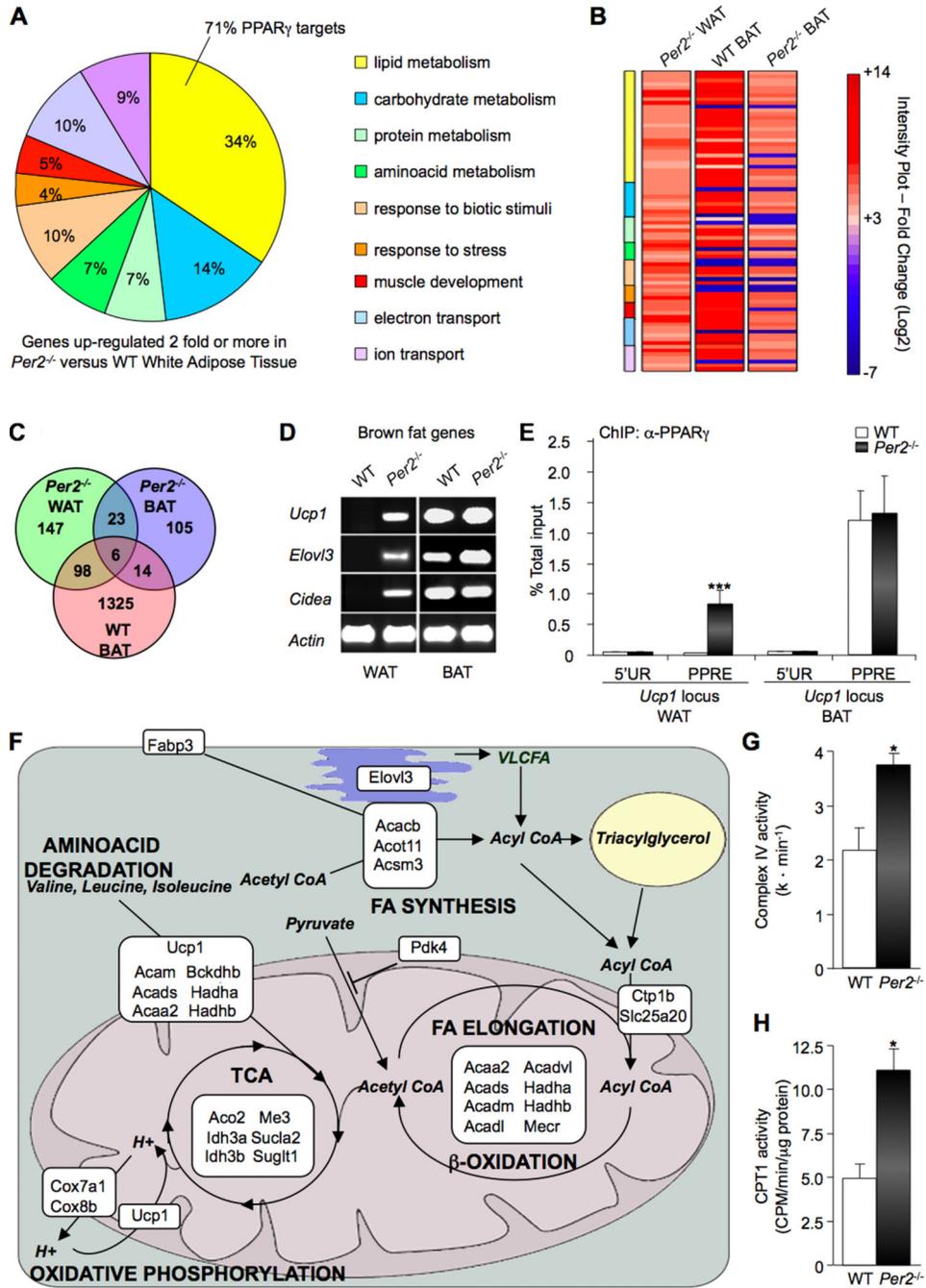
Fig 4. *Per2* **deletion leads to activation of PPARγ-dependent BAT genes in WAT**
(A) Functional classification of microarray data for the most significant upregulated genes in WAT from *Per2*^{-/-} versus WT mice (PPDE>0.995). Percentage of genes sharing common biological processes is presented. Specific PPARγ-target genes in the lipid metabolism group are listed in Table S2. (B) Heat map comparison of significant upregulated genes in WAT from *Per2*^{-/-} mice (*Per2*^{-/-} WAT) with their expression in WT BAT and *Per2*^{-/-} BAT. Expression values are presented as Log2 scale using different gradation of red color for genes upregulated 2-fold or more (Log2 ≥ 1), gray color for genes with fold change between

-2 and +2 (-1 <Log2> +1), and blue color for genes down-regulated 2-fold or more (Log2 -1). Additional information is listed in Tables S2-S7. (C) Venn diagram illustrating overlapping upregulated genes in *Per2*^{-/-} WAT (green), *Per2*^{-/-} BAT (blue) and WT BAT (red). (D) RT-PCR *Per2*^{-/-} BAT brown fat genes *Ucp1*, *Elovl3* and *Cidea* in the WAT and BAT from *Per2*^{-/-} and WT mice. (E) ChIP assay on WAT and BAT nuclear extracts. Chromatin samples were IPed with a α-PPARγ antibody and recovered DNA was analyzed by qPCR with specific primers for the *aP2* locus region flanking the PPRE or an unrelated upstream region (5′UR). Data are presented as percentage of total input. (***$P<0.001$). (F) Schematic representation showing cellular localization and metabolic pathways of the products encoded by upregulated genes in WAT from *Per2*^{-/-} mice. Gene full names and information are listed in Table S8. (G) Complex IV activity in *Per2*^{-/-} and WT WAT. Shown as mean of activity (k * min^{-1}) (*$P<0.05$). (H) CPT1 activity in *Per2*^{-/-} and WT WAT. Shown as mean of activity (CPM/min/μg of protein) (*$P<0.05$).
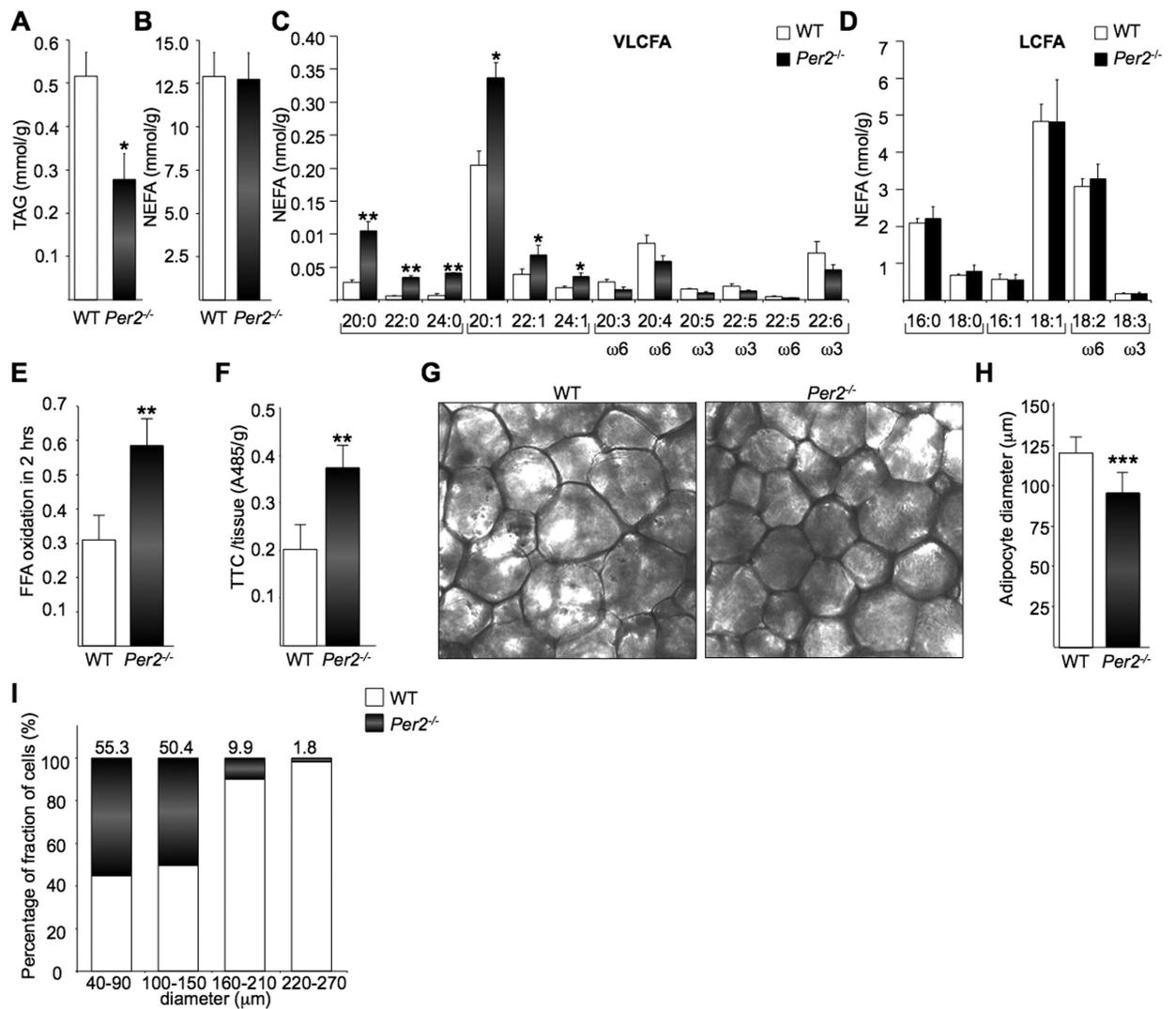
Fig 5. *Per2^{-/-}* mice present an altered lipid profile and increased oxidative capacity in WAT
(A-D) LC/MS analysis of TGA levels comparing WAT from *Per2^{-/-}* and WT mice (A),
NEFA (B), total saturated (SFA), monounsaturated (MUFA), polyunsaturated (PUFA) very
long chain (VLCFA) (C) and long chain fatty acids (LCFA) (D). (*$P < 0.05$; **$P < 0.01$).
(E) and (F) FFA oxidation in adipocytes was measured by $^{14}CO2$ released after 2h of
incubation with ^{14}C-palmitate and TTC staining. (G) Adipocytes cell size measured on dark-
field images of paraformaldehyde-fixed sections of epidydimal adipose tissue. (H) Average
cells diameter is shown in (G) (***$P < 0.001$). (I) Relative percentage of fraction of cells
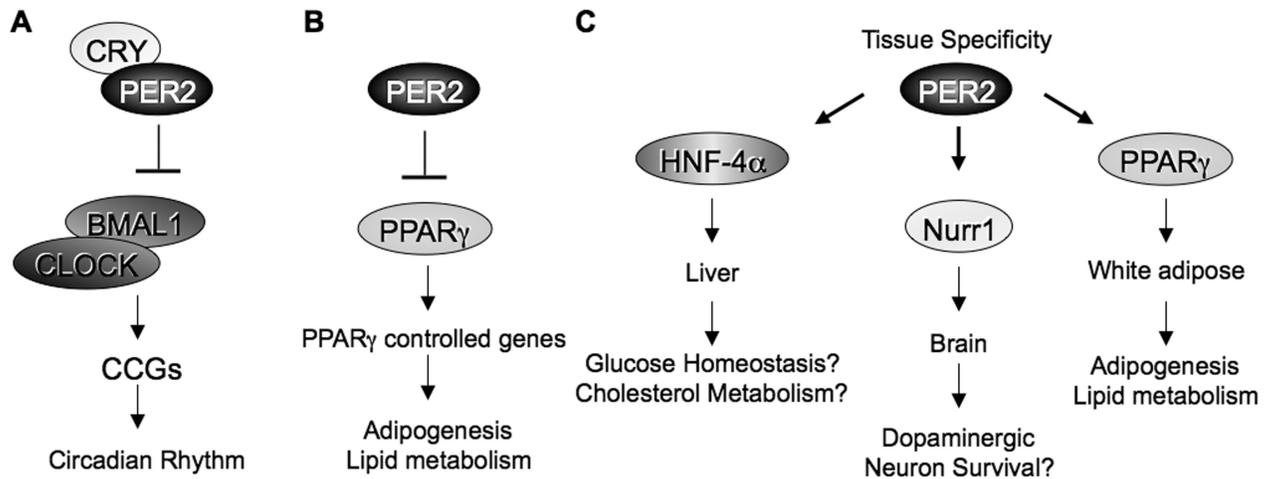with different diameters.

Fig 6. Distinct pathways regulated by PER2

(A) Classical view of PER2 association with CRY to repress CLOCK:BMAL1-directed transcription to control circadian rhythms. (B) Here we have shown that PER2 functions as a critical metabolic regulator by repressing, in a CRY-independent manner, PPARγ-mediated activation of genes involved in adipogenesis and lipid metabolism. (C) We envisage that PER2 may contribute to the regulation of other pathways by specific interactions with selected, tissue-specific transcription factors.